UCRL-17854
c. 2

University of California

Ernest O. Lawrence Radiation Laboratory

MAGNETIC RESONANCE IN ORIENTED NUCLEI

D. A. Shirley

September 1967

TWO-WEEK LOAN COPY

This is a Library Circulating Copy which may be borrowed for two weeks. For a personal retention copy, call Tech. Info. Division, Ext. 5545

UCRL-17854 c. 2

DISCLAIMER

This document was prepared as an account of work sponsored by the United States Government. While this document is believed to contain correct information, neither the United States Government nor any agency thereof, nor the Regents of the University of California, nor any of their employees, makes any warranty, express or implied, or assumes any legal responsibility for the accuracy, completeness, or usefulness of any information, apparatus, product, or process disclosed, or represents that its use would not infringe privately owned rights. Reference herein to any specific commercial product, process, or service by its trade name, trademark, manufacturer, or otherwise, does not necessarily constitute or imply its endorsement, recommendation, or favoring by the United States Government or any agency thereof, or the Regents of the University of California. The views and opinions of authors expressed herein do not necessarily state or reflect those of the United States Government or any agency thereof or the Regents of the University of California.

Invited paper for Conference on Hyperfine Interactions Detected by Nuclear Radiation, August 25-30, 1967, Asilomar, California.

UCRL-17854
Preprint

UNIVERSITY OF CALIFORNIA

Lawrence Radiation Laboratory
Berkeley, California

AEC Contract No. W-7405-eng-48

MAGNETIC RESONANCE IN ORIENTED NUCLEI

D. A. Shirley

September 1967

MAGNETIC RESONANCE IN ORIENTED NUCLEI

D. A. Shirley

Lawrence Radiation Laboratory
University of California
Berkeley, California

September 1967

I. INTRODUCTION

Several new types of experiment that entail radiative detection of nuclear magnetic resonance are discussed in this chapter. The very fact that significant progress in this area is being made simultaneously through diverse experiments in several laboratories demonstrates the rapid growth and potential of radiative detection. At the same time the basic similarity of all these experiments may easily be obscured, largely because the formal theoretical descriptions of the various methods are historically slightly different. It is too early, and probably unnecessary, to make a systematic outline of the many experiments that can be done combining NMR and radiative detection. To stress their basic similarity is, however, the first objective of this paper. It is treated in Sec. II. A brief survey of radiative detection of magnetic resonance in nuclei oriented by equilibrium methods at very low temperatures (NMR/ON) is given in Sec. III. Section IV contains a critical discussion of the hyperfine enhancement factor. Line shapes and "resonance destruction" are treated in Sec. V, and in Sec. VI spin temperatures and spin-lattice relaxation are discussed.

II. RADIATIVE DETECTION OF RESONANCE

In Fig. 1 the various methods for radiative detection of NMR are displayed in a format that emphasizes their similarities. Each method can be divided into three essential steps:

1. Preparation of a nuclear sample in which the magnetic substates of a radioactive level are unequally populated and energetically nondegenerate. This is accomplished through detection of a preceding radiation in the case of NMR/PAC, through low temperatures and a spatially anisotropic Hamiltonian in the NMR/ON method, etc.

2. Radiofrequency irradiation of the sample.

3. Observation of resonance absorption through the frequency dependence of a counting rate.

Beyond the obvious superficial similarity the different experiments have a very basic connection. This is easily understood by considering, for each experiment, a statistical ensemble of samples at time $t = 0$, immediately after preparation (step 1 above). For $t \geq 0$ this ensemble can be fully described by a density matrix. For the common case of a diagonal density matrix the angular properties of the system are conveniently described by statistical tensors B_k familiar from nuclear orientation theory,

$$B_k(t=0) = [(2I+1)(2k+1)]^{1/2} \sum_m (-1)^{I-m} \begin{pmatrix} I & I & k \\ m & -m & 0 \end{pmatrix} \rho_{mm}(t=0), \qquad (1)$$

where ρ_{mm} is a diagonal element of the density matrix. The angular distribution at $t = 0$ is given by

$$W(\theta,t=0) = \sum_k B_k(t=0)\, F_k(LI'I)\, P_k(\cos\theta) \qquad (2)$$

where $F_k(LI'I)$ coefficient familar from angular correlation theory. Here L is the multipolarity of the radiation to be emitted, I is the spin of the state under study, and I' is the final state in the cascade I(L)I'. Once $\rho(0)$ is initially specified, theoretical treatment of the first three cases in Fig. 1 consists simply of evaluating $W(\theta,t)$. For the Mössbauer case polarization of source and absorber must also be considered.

A detailed discussion of the time-development of $W(\theta,t)$ is beyond the scope of this paper, but a few general comments may prove useful. First, an exponential decay factor $e^{-t/\tau}$ clearly attenuates $W(\theta,t)$ in each case (τ is the lifetime of the nuclear state). If relaxation times T_1 and T_2 in the sample are long compared with either τ, or the "time window", Δt, during which observations are made following a beam pulse or an rf pulse, or both, then the theoretical treatment of $W(\theta,t)$ remains identical even in the presence of RF fields. This follows because each nucleus can be regarded as independent.

Spin-spin interactions between identical nuclei are important only in the NMR/ON and NMR/Mössbauer experiments, because in the NMR/PAC and NMR/NR cases the excited states are only present essentially "one at a time." Of course even for the former two cases spin-spin interaction can usually be made negligible by dilution.

In the NMR/PAC and NMR/Mössbauer methods nuclear decay is the "alternative process" with which NMR absorption must compete, and the ultimate linewidth is given by the nuclear lifetime. In the NMR/ON and NMR/NR cases either nuclear decay or spin-lattice (T_1) relaxation (or both) may determine the time available

for NMR absorption. In either of these latter two cases this time interval is likely to be longer and linewidths consequently narrower, than in the former two cases.

It should be noted that T_1 in a metal varies inversely with temperature. For light atoms T_1T is of the order of 1(sec-deg K), while for heavy atoms $T_1T \sim 10$ (msec-deg K). Thus T_1 provides an upper limit[1] on the available time for measurement in an NMR/NR experiment, if τ is in the millisecond range and the catcher foil is at the ambient temperature. Larger effects and narrower lines, as well as extension to longer halflives, will be attainable using catcher foils refrigerated to liquid helium temperatures.

III. SURVEY OF RESULTS TO DATE

In 1953 Bloembergen and Temmer suggested[2] that magnetic resonance on oriented nuclei would provide accurate measurements of hyperfine structure constants. Unfortunately the experiments that they suggested, on paramagnetic salts, were apparently not feasible, and early attempts to observe a resonance effect on the angular distribution of radiation failed[3] because of excessive heating at nonresonant frequencies. Thirteen years elapsed before Matthias and Holliday reported[4] the first successful experiment below 1°K,[5] on ^{60}Co oriented in iron. Templeton and Shirley expanded[6] the technique to include frequency modulation and to measure T_1 for ^{60}Co and ^{54}Mn in Fe. Barclay et al., have observed[7] the resonance for ^{125}Sb in Fe. Niesen, Lubbers, and Huiskamp have observed[8] resonance in a paramagnetic sample, ^{54}Mn in lanthanum magnesium nitrate. These workers have thus done an experiment that is superficially quite similar to

the original Bloembergen-Temmer proposal, though, as they point out,[8] with the crucial differences of high magnetic field, magnetic dilution, and radiofrequency radiation at a low power level. This low power level is sufficient to induce transitions because of amplification through hyperfine enhancement, discussed below.

IV. HYPERFINE ENHANCEMENT: A CRITIQUE

"Ferromagnetic enhancement" which made possible the first experiments combining NMR with perturbed angular correlations,[9] nuclear orientation,[4] and Mössbauer spectroscopy,[10,11] and "paramagnetic enhancement," which was used by Niesen, et al.,[8] are special cases of the more general phenomenon of "hyperfine enhancement," well-known in atomic spectroscopy.[12,13] In the discussion that follows it is shown that this enhancement is a necessity in some experiments, while for others it may actually be disadvantageous.

First let us recall the usual description of a magnetic resonance experiment, referring to Fig. 2. We have a system with angular momentum I and magnetic moment $\mu = \gamma I$, a static field $\vec{H}_0$ directed along the z axis, and an oscillatory field $H_1(t) = 2H_1 \cos \omega t$ directed along the x axis. The motion of μ follows from the torque equation $\frac{d\vec{\mu}}{dt} = \gamma\vec{\mu} \times \vec{H}_0$, i.e., $\vec{\mu}$ precesses about H_0 with a frequency $\omega_0 = \gamma H_0$. Transforming into the Larmor frame, we find that H_0 has disappeared, and $\vec{\mu}$ is no longer precessing about the z axis. The oscillatory field $H_1(t)$ may be resolved into its two circularly polarized components, for $\omega = \omega_0$ the component with the correct sense will appear in the Larmor frame as a constant field along the x axis. The NMR process may be understood as precession about this field.

In a radiative detection-NMR experiment it is desirable to induce at least one transition in each nucleus in the lab frame, which amounts to precession of ~1 radian about H_1 in the Larmor frame. Thus the effective oscillatory field, H_1, must be sufficiently large that $\omega_1\tau_c \sim 1$, where $\omega_1 = \gamma H_1$ is the precession frequency in the Larmor frame, and τ_c is the correlation time (i.e., T_1 or $T_{1/2}$) which is essentially the time available for observation.

The field strength H_1 of the oscillatory field at the nucleus is stronger than the applied field $H_1^{(app)}$ by the enhancement factor F. The electron spins can follow $H_1^{(app)}$ almost adiabatically (the NMR frequency being much lower than that for ferromagnetic resonance). Thus F is practically the same as for an applied static field, i.e.,

$$H_0 = FH_0^{(app)} = H_0^{(app)} + H_{hf}$$

$$\therefore \quad F = 1 + H_{hf}/H_0^{(app)}, \quad \text{and} \tag{3}$$

$$H_1 = FH_1^{(app)} = (1 + H_{hf}/H_0^{(app)})\, H_1^{(app)}.$$

Applying the criterion $\omega_1\tau_c > 1$, we find $H_1^{(app)}/H_0^{(app)} > (\omega_0\tau_c)^{-1}$ as the criterion for the necessary applied radiofrequency field strength.

Applying these results to a nuclear orientation experiment with $H_0^{(app)} = 10^3$ G, $\omega_0 = 10^9$ Hz, and $T_1 = 10^2$ sec, we find that an $H_1^{(app)}$ of only 10^{-8}G is needed. If the situation were really this simple then NMR/ON would be a very easy technique indeed, and would be immediately applicable to many systems. Unfortunately this estimate involves the implicit assumption that a natural

linewidth of $\lambda \sim T_2^{-1} \sim 10^{-2}$ Hz is attainable. In ferromagnetic metals a more typical linewidth is $\Gamma \sim 10^6$ Hz, because of inhomogeneous broadening. Thus a radiofrequency field can resonate all the nuclei within a frequency interval λ, but these constitute only a fraction $\lambda/\Gamma \sim 10^{-8}$ of the nuclear species under study. Of course frequency modulation over a bandwidth $\Delta\nu > \lambda$ will allow a fraction $\Delta\nu/\Gamma$ of the nuclei to be reached, but the duty cycle then drops to $\lambda/\Delta\nu$, and the amplitude of the external radiofrequency field H_1^{ext} must be increased accordingly. Clearly it is necessary, in order to resonate all the nuclei in an inhomogeneously broadened line of width $\Gamma = 10^6$ Hz, to apply an effective time-averaged field $H_1^{(app)} \sim 10^{-8}$G at each frequency. If $\lambda \sim 10^{-2}$ Hz is the natural linewidth, then this requires a frequency-modulated external field of bandwidth Γ and strength $H_1^{ext} = 1$ G. At this level radiofrequency heating becomes appreciable. This constitutes the most serious present limitation for the NMR/ON method as applied to ferromagnetic metals.

One way to overcome this difficulty is to reduce the inhomogeneous broadening. This may be done by improving the purity of the specimen and particularly by using single crystals. In Fig. 3 the NMR spectra from Co^{60} oriented in a single crystal of iron and in polycrystalline iron are compared. Neither of these lines represents the best possible experimental conditions. With polycrystalline sources lines as narrow as 600 kHz have been obtained, and the single crystal used here was only 99.7% pure. Still the qualitative conclusion is obvious: narrower lines are possible in single crystals.

Another way to reduce inhomogeneous broadening in metals is to use an external magnetic field directly, rather than the hyperfine fields in ferromagnets, to split the nuclear magnetic substates. The narrower linewidth in a

nonferromagnetic metal ($\Gamma \sim 10^3$ Hz, rather than 10^6 Hz) essentially compensates for the absence of a hyperfine enhancement factor. Thus a ferromagnetic host is unnecessary. In fact nonmagnetic metals are clearly preferable for magnetic moment determinations ($\nu/\Gamma \sim 10^5$, rather than $\sim 10^3$), and by using both magnetic and nonmagnetic lattices hyperfine-anomaly determinations are also possible.

V. RESONANT DESTRUCTION AND INTRINSIC MULTIPOLE STRUCTURE

The NMR/ON method has been referred to as "resonant destruction" of nuclear orientation. In fact, as Matthias and Olsen have found[14] for angular correlation, complete destruction of the anisotropic components of angular distribution on resonance is possible only for odd spherical harmonics. It is convenient in nuclear orientation problems to approach this problem from a slightly different point of view. The angular distribution of radiation from an assembly of oriented nuclei is given in the absence of an rf field by

$$W(\theta) = \sum_k A_k P_k (\cos \theta), \tag{4}$$

where P_k is a Legendre polynomial of order k, and θ is the angle from the hyperfine field direction. At resonance it is convenient to consider the problem in the Larmor frame, where this distribution precesses around H_1 (i.e., in the yz plane, around the x axis). If we had detectors in the Larmor frame we would find that the time-integrated intensity would be given everywhere in the yz plane by

$$W_{yz} = \sum A_k \overline{P}_k \quad , \tag{5}$$

where

$$\overline{P}_k = \frac{\int_0^k P_k(\cos\theta)\, d\theta}{\int_0^\pi d\theta} = [P_k(\cos \pi/2)]^2 \quad . \tag{6}$$

For k = 0 through 6, $\overline{P}_k$ is respectively 1, 0, 1/4, 0, 9/64, 0, and 25/256. In practice, of course, the radiation detectors are in the laboratory frame. At $\theta = 0$, however, these frames coincide and the time-average of the attenuation coefficient G_k is given by $\overline{G}_k = [P_k(\cos \pi/2)]^2$ for observation along the z axis in the laboratory frame, i.e., $W(\theta_{lab} = 0) = \sum_k A_k G_k P_k(0) = \Sigma A_k [P_k(\cos \pi/2)]^2$. In fact G_k is independent of θ. Thus there are non-zero hard-core values for all even-rank statistical tensors at the resonant frequency, and total resonant destruction is not possible. It should be noted that these results apply only for the limiting case $\tau_c \omega_0 \to \infty$, and $T_{1/2}\, \omega_0 \to \infty$: introduction of finite correlation times and/or halflife will modify these results.

An "intrinsic multipole structure" should be present in magnetic resonance lines detected through tensors of higher than first rank. For a kth-rank tensor this effect is manifest as a k-plet of components symmetrically disposed about the central frequency. This result can be derived in serveral ways. For angular correlations Matthias and Olsen have shown[14] it by direct calculation. It can be qualitatively appreciated by imagining an angular distribution $W(\theta)$, as in Eq. (4), rotating in the Larmor frame but not in the (rotating) xy plane, because off resonance the (laboratory) static field does not go to zero in the Larmor frame. The statistical tensors must therefore precess (in the Larmor frame) about the resultant of the oscillatory field H_1 and the remanent static field, $H_o \frac{\omega-\omega_o}{\omega_o}$. It is easy to see how the multipole structure arises as ω is varied away from ω_0.

Multipole structure is also implicit in the "Majorana Factors", $P_{mm'}(t)$ which are elements of a probability matrix given[15] by Majorana. Here $P_{mm'}(t)$ is the probability that a nucleus starting in magnetic substate $|m\rangle$ at time zero will be in substate $|m'\rangle$ at time t. Both $|m\rangle$ and $|m'\rangle$ are magnetic eigenstates in the laboratory frame. The analytic expression for $P_{mm'}(t)$ is

$$P_{mm'}(t) = (\cos \alpha/2)^{4I} \, (I+m)! \, (I+m')! \, (I-m)! \, (I-m')!$$

$$\times \left[\sum_{n=0}^{2I} \frac{(-1)^n \, (\tan \alpha/2)^{2n-m+m'}}{n! \, (n-m+m')! \, (I+m-n)! \, (I-m'-n)!} \right]^2 . \tag{7}$$

Here α is defined by $\sin^2\alpha/2 = \sin^2\theta \, \sin^2 at/2$, where θ is the angle between $\vec{H}_0$ and the effective field in the Larmor frame. This effective field is the vector sum of $\vec{H}_1$ and the remanent static field in the Larmor frame, $(H_0 + \omega/\gamma) \, \vec{H}_0/|H_0|$, where H_0 is the static field in the laboratory frame. The parameter a is given by $a = - [(\omega_0-\omega)^2 + \omega_1^2] \, \gamma/|\gamma|$.

The effective nuclear-orientation statistical tensors at time t and in the laboratory frame $B_k(t)$ may be written

$$\begin{aligned} B_k(t) &= G_k(t) \, B_k(0) \\ &= [(2I+1)(2k+1)]^{1/2} \sum_{mm'} (-1)^{I-m'} \begin{pmatrix} I & I & k \\ m & -m & 0 \end{pmatrix} \rho_{mm}(0) \, P_{mm'}(t) . \end{aligned} \tag{8}$$

In most nuclear-orientation experiments the nuclear lifetime is much longer than ω_1^{-1}, and $\overline{G_k(\infty)}$, the effective integral value of $G_k(t)$, is obtained

by integrating $P_{mm'}(t)$ over $e^{-t/\tau}$, and letting $\tau \to \infty$; i.e.,

$$\overline{P_{mm'}(\infty)} = \lim_{\tau \to \infty} 1/\tau \int_0^\infty P_{mm'}(t)\, e^{-t/\tau}\, dt \quad . \tag{9}$$

From Eqs. (7) - (9) we may calculate $\overline{G_k(\infty)}$ as a function of ω/ω_0 for any value of H_1/H_0. Typical results are shown for k = 1 and 2, respectively, in Figs. 4 and 5. Four features of these curves should be noted:

1. The hard core values are as predicted.

2. The intrinsic multipole structure stands out. Experimental determination of the values of ω/ω_0 corresponding to the zeroes of $\overline{G_k(\infty)}$ would give directly the effective values of H_1 in the Larmor frame.

3. The lines are not simply Lorentzian for $k > 1$.

4. As shown in Sec. II, these results apply equally well to the nuclear reaction and angular correlation cases.

VI. SPIN-LATTICE RELAXATION AND SPIN TEMPERATURE

Time-dependent effects were observed in early experiments on Co^{60} in iron, arising from a spin-lattice relaxation time, T_1, of the order of one minute. To measure T_1 accurately, Templeton and Shirley directed the signal from a γ-ray detector placed along the polarization direction of a Co^{60}-in-iron source to a multiscalar, obtaining the type of curve shown in Fig. 6. During a run the radiofrequency power level was maintained constant throughout, to avoid spurious heating effects. The curve in Fig. 6 may be regarded as consisting of five parts. During intervals A and E, which correspond to "foredrifts" and "afterdrifts" in calorimetry, the spin and lattice systems are at a common temperature, and any change in the counting rate (which serves as the thermometer) arises from heat leak (including rf heating) into the combined system. During intervals A, D, and E the RF radiation is slightly off-resonance and is unmodulated. At the beginning of interval B the rf frequence is moved to the resonance region and is swept through resonance repeatedly during intervals B and C. Interval B is defined as the "buildup" period during which the spin temperature T_s reaches a steady state value T'_s much higher than that of the lattice, T_L. After steady state has been established, as evidenced by the constancy of T'_s, the rf frequency is shifted from resonance, and the nuclei relax to the lattice temperature, in region D. Three assumptions were made for the interpretation of the first <u>Fe</u> Co^{60} experiments, all three of which were supported for that case by direct calculation:

1. A spin temperature T_s exists.
2. The equation $\frac{d}{dt}\left(\frac{1}{T_s}\right) = -\frac{1}{T_1}\left[\frac{1}{T_s} - \frac{1}{T_L}\right]$ is approximately correct.
3. The orientation tensor B_2 varies as $a + b(1/T_s)$ in the region of interest.

With these assumptions we can write

$$W(\theta,t) - W(\theta)_{eq} = [W(\theta,0) - W(\theta)_{eq}]e^{-t/T_1} \tag{10}$$

for the time dependence of the γ-ray intensity at angle θ. Neither of the latter two assumptions are generally valid, and it is useful to have an exact expression for the time dependence of $W(\theta)$. This is most readily done by calculating the time dependence of $(1/T_s)$ by the method shown below.

Consider an assembly of identical nuclei with spin I under an "effective field" Hamiltonian that lifts the degeneracy of the magnetic substates, giving $2I + 1$ sublevels separated by energy $h\nu = \gamma H$ and labelled in order from the top by the (good) quantum number $m = I, I - 1, \ldots, -I$. Suppose that the spin temperature is higher than that of the lattice, $T_s > T_L$, or $x' > x$, where $x = h\nu/kT_s$ and $x' = h\nu/kT_L$. The spin system loses internal energy at the rate

$$\frac{dU}{dt} = Nh\nu \sum_m [P(m+1 \rightarrow m) - P(m \rightarrow m+1)] \tag{11}$$

where N is the number of nuclei present and $P(m \rightarrow m')$ is the probability per unit time that any nucleus will experience a transition from $|m\rangle$ to $|m'\rangle$. Invoking microscopic reversibility, separating the m-dependence of the transition probabilities from the "reduced" probability $W_0 = 1/2T_1$, and denoting by a_m the probability of any nucleus being in state $|m\rangle$, we have

$$\frac{dU}{dt} = Nh\nu\, W_0 \sum_m [I(I+1) - m(m+1)] \left(a_{m+1} - a_m e^{-x'}\right) \tag{12}$$

Since $a_{m+1} = a_m e^{-x}$, this becomes

$$\frac{dU}{dt} = Nh\nu\, W_0\left(e^{-x} - e^{-x'}\right) \sum_{m=-I}^{I-1} [I(I+1) - m(m+1)]\, a_m \quad . \tag{13}$$

After some algebra this becomes

$$\frac{dU}{dt} = Nh\nu\, W_0\left(e^{-x} - e^{-x'}\right)\frac{\sinh x/2}{\sinh(I+1/2)x} \sum_{-I}^{I-1} [I(I+1) - m(m+1)]e^{-mx} \quad . \tag{14}$$

It is readily shown from the definition of U for this system that

$$\frac{dU}{dx} = Nh\nu[\langle m\rangle^2 - \langle m^2\rangle] \quad . \tag{15}$$

Therefore

$$\frac{dx}{dt} = \frac{\left(e^{-x} - e^{-x'}\right)}{2T_1\left[\langle m\rangle^2 - \langle m^2\rangle\right]} \frac{\sinh x/2}{\sinh(I+1/2)x} \sum_{-I}^{I-1} [I(I+1) - m(m+1)]e^{-mx} \tag{16}$$

gives the time-dependence of x. We may integrate with suitable boundary conditions to find $T_s(t)$. It is also useful to work with the time-dependences of the more directly measureable quantities $B_k(x)$. For B_2 for example we have the exact expression

$$\frac{dB_2}{dt} = \frac{3(e^{-x}-e^{-x'})}{2T_1\,[\frac{1}{5}I(I+1)(2I-1)(2I+3)]^{1/2}} \; \frac{\langle m\rangle\langle m^2\rangle-\langle m^3\rangle}{\langle m\rangle^2-\langle m^2\rangle} \tag{17}$$

$$\times \quad \frac{\sinh x/2}{\sinh(I+1/2)x} \sum_{-I}^{I-1} [I(I+1) - m(m+1)]e^{-mx} \quad .$$

For any set of boundary conditions x' and x(t=0), this expression may readily be integrated. A typical curve is shown in Fig. 7, for I = 7/2.

Two other topics of interest in connection with T_1 studies may be mentioned. First the NMR/ON method allows us to explore a new region of spin temperatures heretofore inaccessible. It is possible to explore rather critically the conditions under which a spin temperature exists. By measuring B_1, B_2, and B_4 simultaneously in a system for which $T_s \gg T_L$ one may, for example, derive various moments of I_z(i.e., $\langle m\rangle$, $\langle m^2\rangle$, $\langle m^4\rangle$) simultaneously. Comparison with the hyperfine Hamiltonian for the system applies stringent criteria for the existence of a unique T_s. In Fig. 8 the variation with x of these three B_k for an assembly of spin-5 nuclei is shown, to illustrate that their measurement would give three quite separate temperature determinations.

The second point is that the Korringa relation T_1T = constant for metals is only a high-temperature approximation and is expected to break down in just the region where nuclear orientation becomes appreciable, namely $x \sim 1$. Cameron, et al., have shown[16] that T_1 is expected to vary as $(1-e^x)/\gamma He^x$. The early results on <u>Fe</u>Co^{60} are compared with a curve of this form in Fig. 9. The beginning of non-linear behavior seems to be present, but extension of these measurements to lower temperatures is desirable.

Intuitive insight into the origin of the constancy of T_1 at low temperatures may be obtained by referring to Fig. 10 and 11, which also illustrate possible applications to Fermi surface studies. In Fig. 10, for $h\nu \ll kT$, it is clear that the transition probability (and T_1^{-1}) for a relaxation process involving the Fermi surface, is proportional to the absolute temperature. This is true because

$$T_1^{-1} \propto \int n_i(1-n_f)dE \propto T, \tag{18}$$

i.e., the initial and final occupation probabilities, n_i and n_f, are essentially equal for $h\nu \ll kT$, and major contributions to the integral arise in an energy region of width $\sim kT$ around the Fermi energy. In Fig. 11 the opposite extreme, $h\nu \gg kT$, is illustrated. Here either n_i or $1 - n_f$ is zero except for a band of width $\sim h\nu$ around E_F. Thus $T_1^{-1} \propto \int n_i(1-n_f)_f\, dE \propto h\nu$, i.e., T_1 is temperature-independent. Clearly the variation of T_1 with T between these two extremes is dependent on the functional behavior of $n(E)$ around the Fermi surface. Careful measurements of $T_1(T)$ could test this functional behavior.

ACKNOWLEDGEMENTS

This work was carried out in part at the Lawrence Radiation Laboratory, Berkeley, supported by the U. S. Atomic Energy Commission, and in part at the Mullard Cryomagnetic Laboratory, Clarendon Laboratory, Oxford, while the author was a National Science Foundation Senior Postdoctoral Fellow.

Several of the ideas mentioned here arose in conversations with Dr. E. Matthias and Dr. J. E. Templeton, and will be more completely developed elsewhere. Mr. W. D. Brewer and Mr. J. A. Barclay assisted in obtaining the single crystal resonance shown in Fig. 3, and Mr. Brewer calculated the curve shown in Fig. 7.

REFERENCES AND FOOTNOTES

1) E. Matthias and D. A. Shirley, Nucl. Instr. Methods 45, 309 (1966).

2) N. Bloembergen and G. M. Temmer, Phys. Rev. 89, 883 (1953).

3) G. M. Temmer, private communication.

4) E. Matthias and R. J. Holliday, Phys. Rev. Letters 17, 897 (1966).

5) F. M. Pipkin and co-workers (Phys. Rev. 106, 1102 (1957); 109, 1423 (1958); 112, 935 (1958); 123, 1824 (1961)) have reported radiative detection of ENDOR in dynamically oriented ^{76}As and ^{122}Sb.

6) J. E. Templeton and D. A. Shirley, Phys. Rev. Letters 18, 240 (1957).

7) J. A. Barclay, W. D. Brewer, E. Matthias, and D. A. Shirley, paper , this volume.

8) L. Niesen, J. Lubbers, and W. J. Huiskamp, paper , this volume.

9) E. Matthias, D. A. Shirley, M. P. Klein, and N. Edelstein, Phys Rev. Letters 16, 974 (1966).

10) G. Perlow, reported in the Urbana Conference on the Mössbaur Effect (1960), and private communication.

11) E. Matthias, preceeding paper.

12) A. M. Portis and R. H. Lindquist, in "Magnetism", Vol. IIA, p. 357 (ed. by G. T. Rads and H. Suhl, Academic Press, 1965).

13) P. Kusch, S. Millman, and I. I. Rabi, Phys. Rev. 57, 765 (1940).

14) E. Matthias and B. Olsen, private communication, August, 1967.

15) E. Majorana, Nuovo Cimento 9, 43 (1932).

16) J. A. Cameron, I. A. Campbell, J. P. Compton, and R. A. G. Lines, Physics Letters 10, 24 (1964).

FIGURE CAPTIONS

Fig. 1. Methods employing radiative detection of NMR, drawn to illustrate their similarity.

Fig. 2. Magnetic resonance fields in laboratory frame and Larmor frame.

Fig. 3. Gamma-ray intensity following the decay of Co^{60} oriented in iron as a function of applied RF frequency.

Fig. 4. Attenuation coefficient for a first-rank statistical tensor averaged over $0 \leq t \leq \infty$, for a nuclear state of very long lifetime, $\omega_1 \tau \gg 1$, for two power levels.

Fig. 5. Attenuation coefficient for a second-rank statistical tensor averaged over $0 \leq t \leq \infty$, for a nuclear state of very long lifetime, $\omega_1 \tau \gg 1$, for two power levels.

Fig. 6. Determination of T_1 from radiation intensity. Regions A and E are fore-and afterdrifts. Radiofrequency radiation goes into the resonant region between A and B, and leaves between C and D.

Fig. 7. Time-dependence of $\Delta B_2 = B_2(T_s) - B_2(T_L)$ for $I = 7/2$.

Fig. 8. Dependence of statistical tensors on the temperature parameter x, illustrating that the simultaneous determination of B_1, B_2, and B_4 for $T_s > T_L$ would be a sensitive criterion for the existence of a unique spin temperature T_s.

Fig. 9. Comparison of temperature dependence of T_1 for $\underline{Fe}Co^{60}$ (Ref. 6) with Korringa approximation and exact theory.

Fig. 10. Fermi surface for $h\nu \ll kT$.

Fig. 11. Fermi surface for $h\nu \gg kT$.

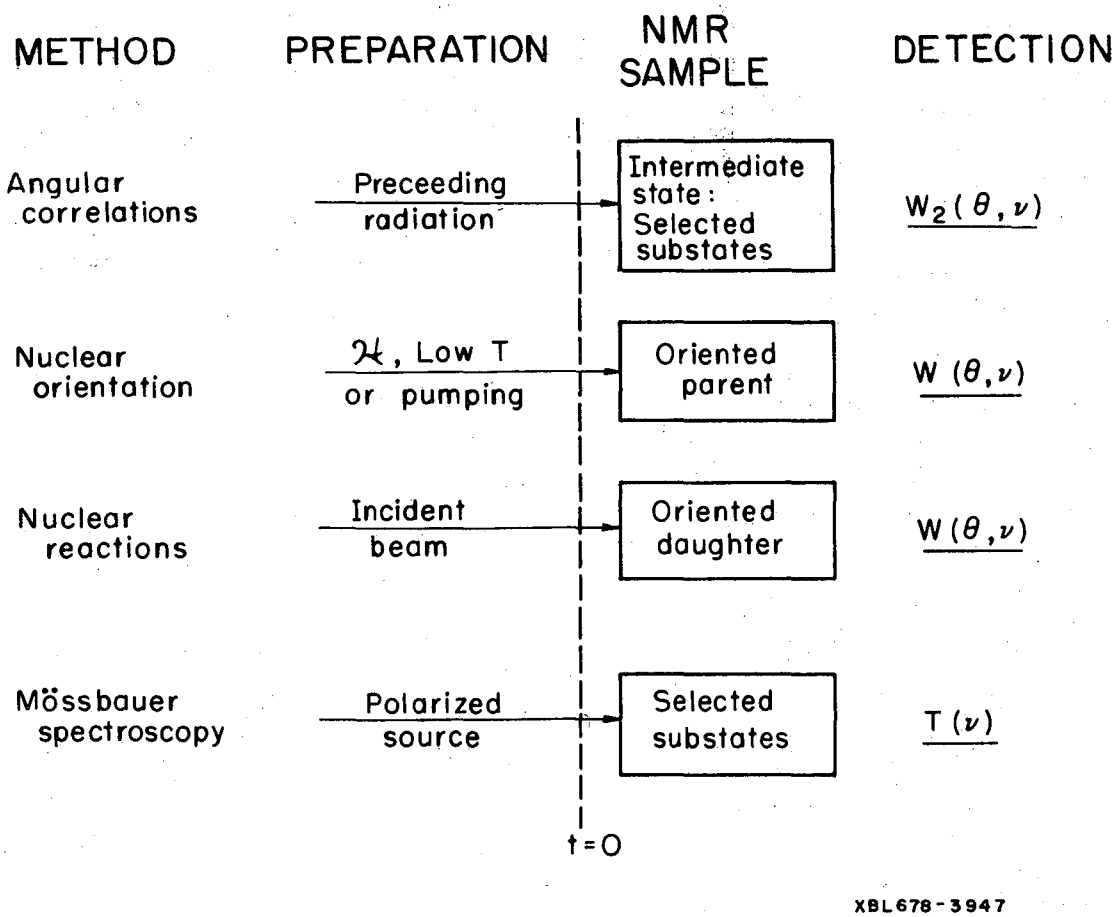
METHOD
PREPARATION
NMR SAMPLE
DETECTION
Angular correlations
Preceeding radiation
Intermediate state: Selected substates
$W_2(\theta, \nu)$
Nuclear orientation
$\mathcal{H}$, Low T or pumping
Oriented parent
$W(\theta, \nu)$
Nuclear reactions
Incident beam
Oriented daughter
$W(\theta, \nu)$
Mössbauer spectroscopy
Polarized source
Selected substates
$T(\nu)$
t=0
XBL678-3947

Fig. 1

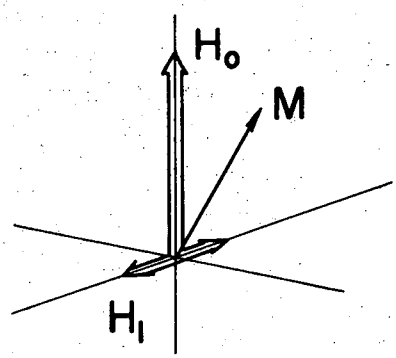

Laboratory Frame

$$\frac{d\mathbf{M}}{dt} = \gamma \mathbf{M} \times \mathbf{H}_o$$

$$\hbar\omega_o = \gamma H_o$$

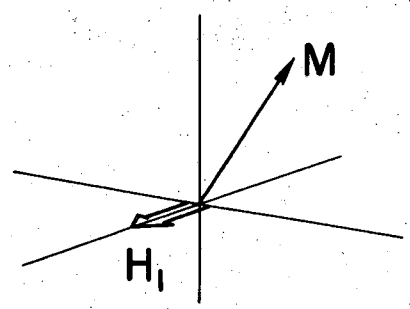

Larmor Frame

$$\frac{d\mathbf{M}}{dt} = \gamma \mathbf{M} \times \mathbf{H}_1$$

$$\hbar\omega_1 = \gamma H_1$$

XBL678-3948

Fig. 2

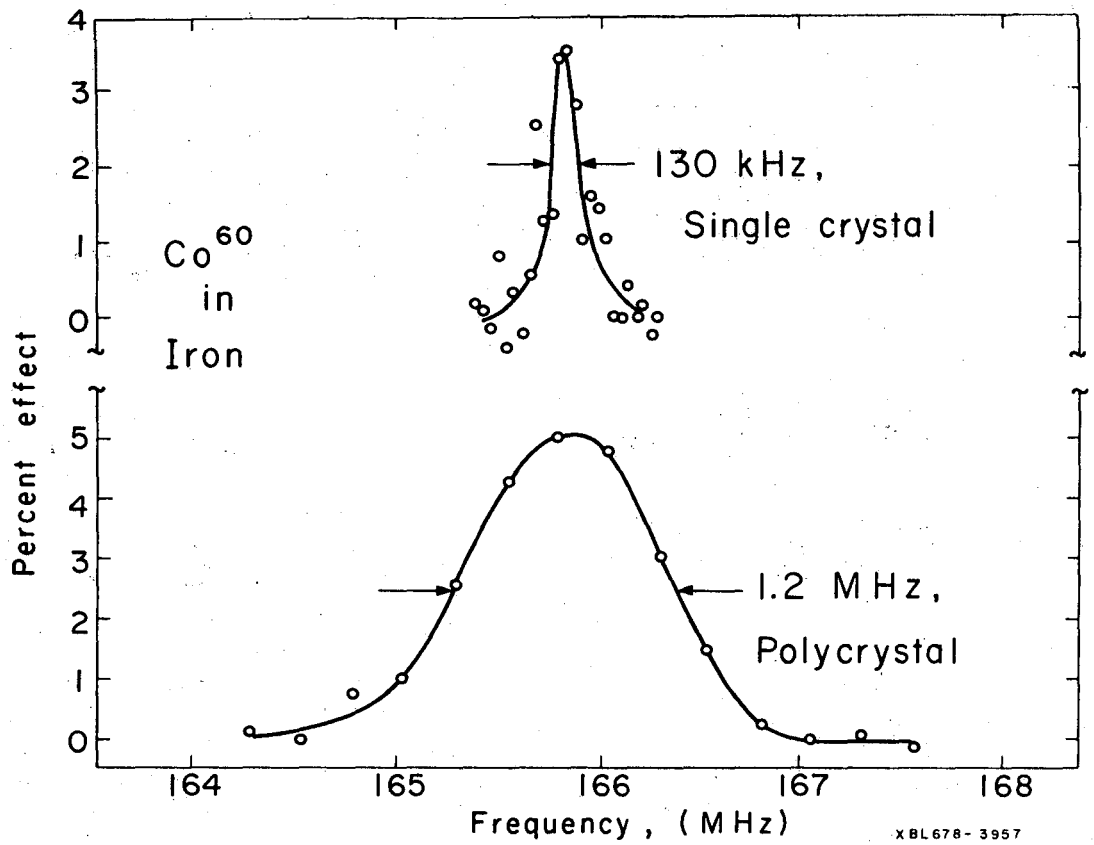
Percent effect
Co60
in
Iron
130 kHz,
Single crystal
1.2 MHz,
Polycrystal
Frequency, (MHz)
XBL678-3957

Fig. 3

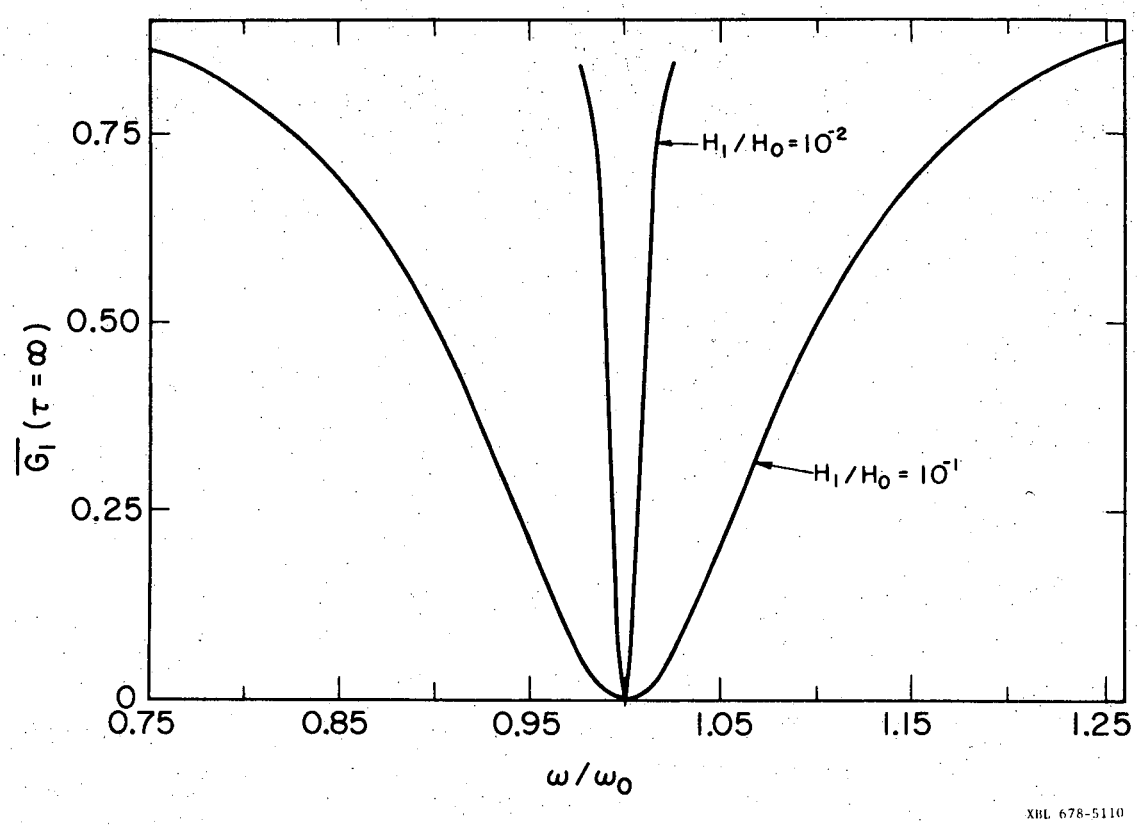
0.75
0.50
0.25
0
$\overline{G_1}(\tau = \infty)$
$H_1/H_0 = 10^{-2}$
$H_1/H_0 = 10^{-1}$
0.75
0.85
0.95
1.05
1.15
1.25
ω/ω_0
XBL 678-5110

Fig. 4

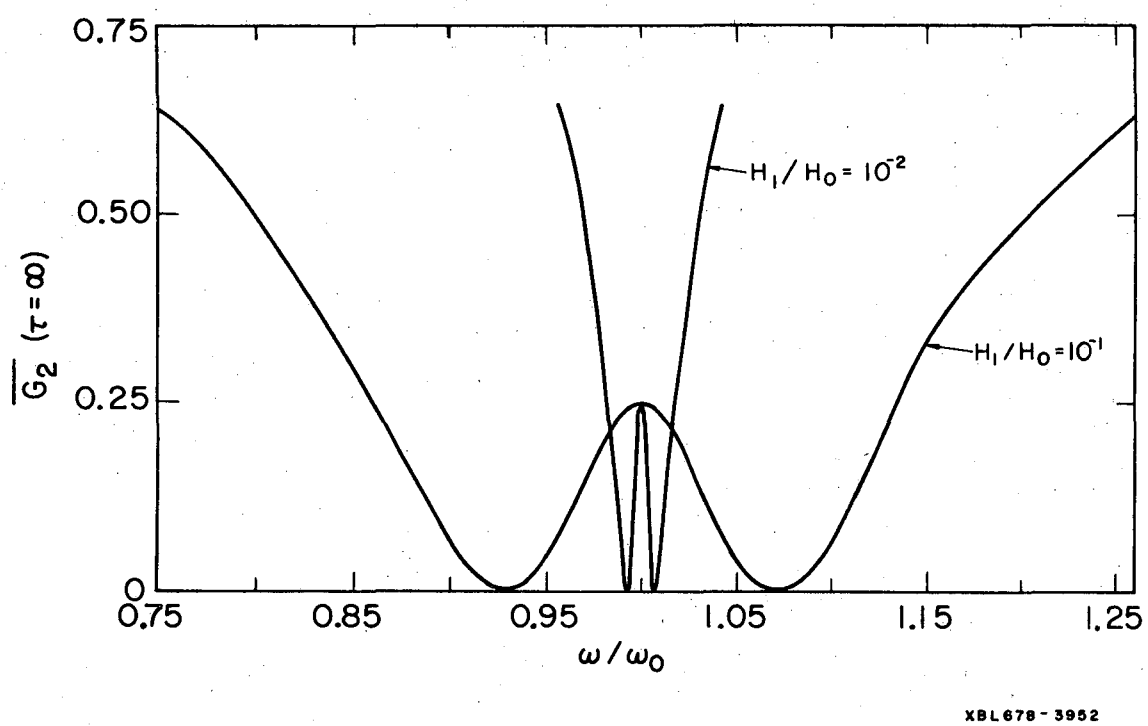
0.75
0.50
0.25
0
$\overline{G_2}$ ($\tau = \infty$)
0.75
0.85
0.95
1.05
1.15
1.25
ω / ω_0
$H_1 / H_0 = 10^{-2}$
$H_1 / H_0 = 10^{-1}$
XBL678-3952

Fig. 5

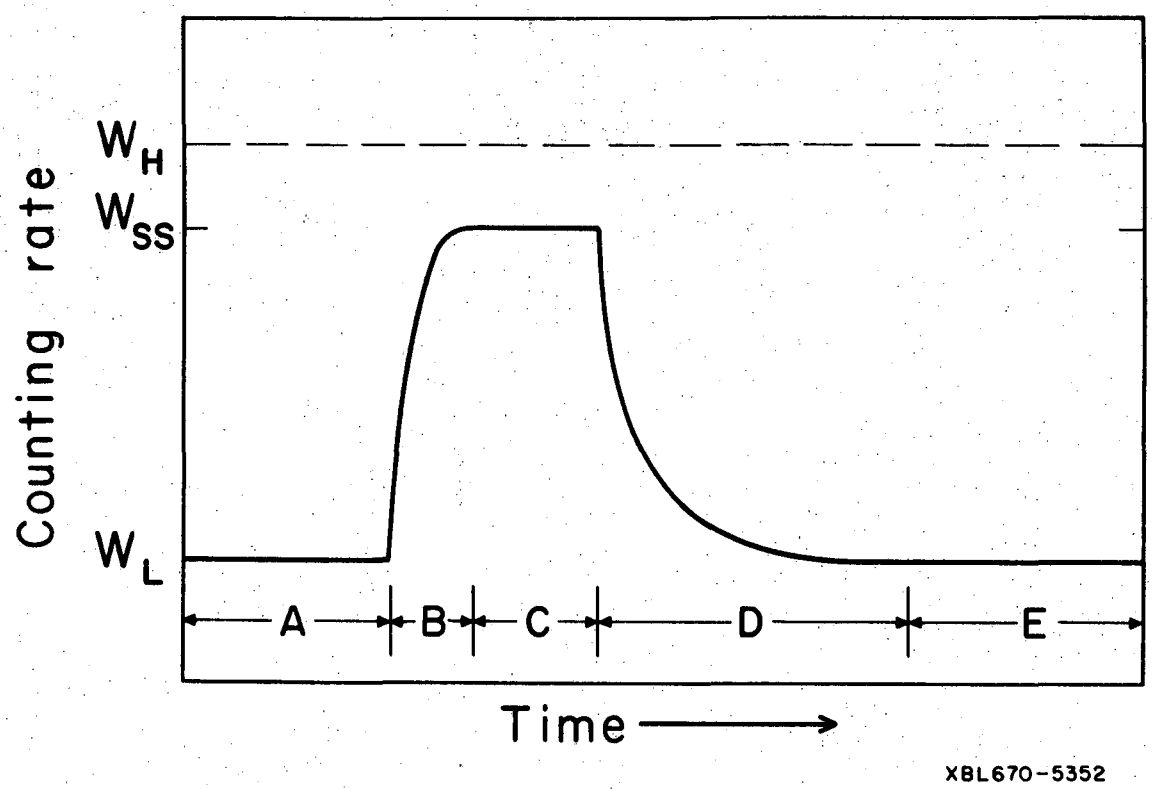

Fig. 6

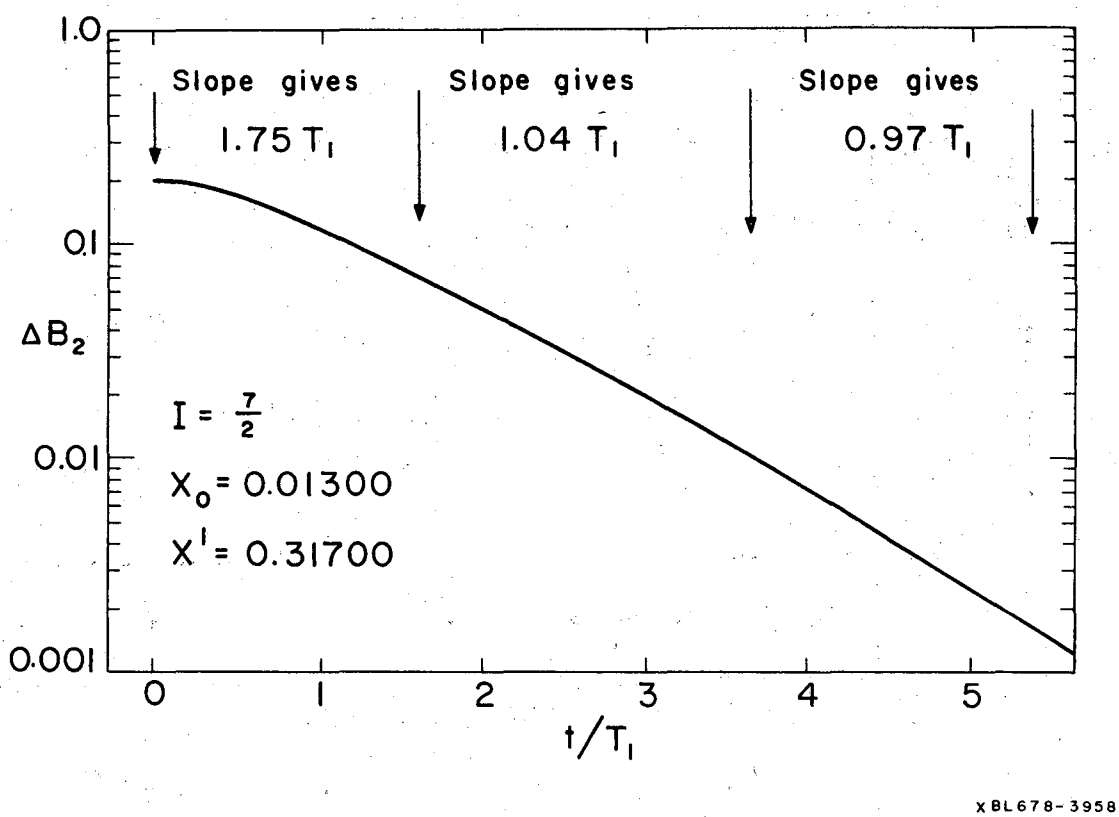
1.0
0.1
0.01
0.001
ΔB2
Slope gives
1.75 T1
Slope gives
1.04 T1
Slope gives
0.97 T1
I = 7/2
X0 = 0.01300
X' = 0.31700
0
1
2
3
4
5
t/T1
XBL678-3958

Fig. 7

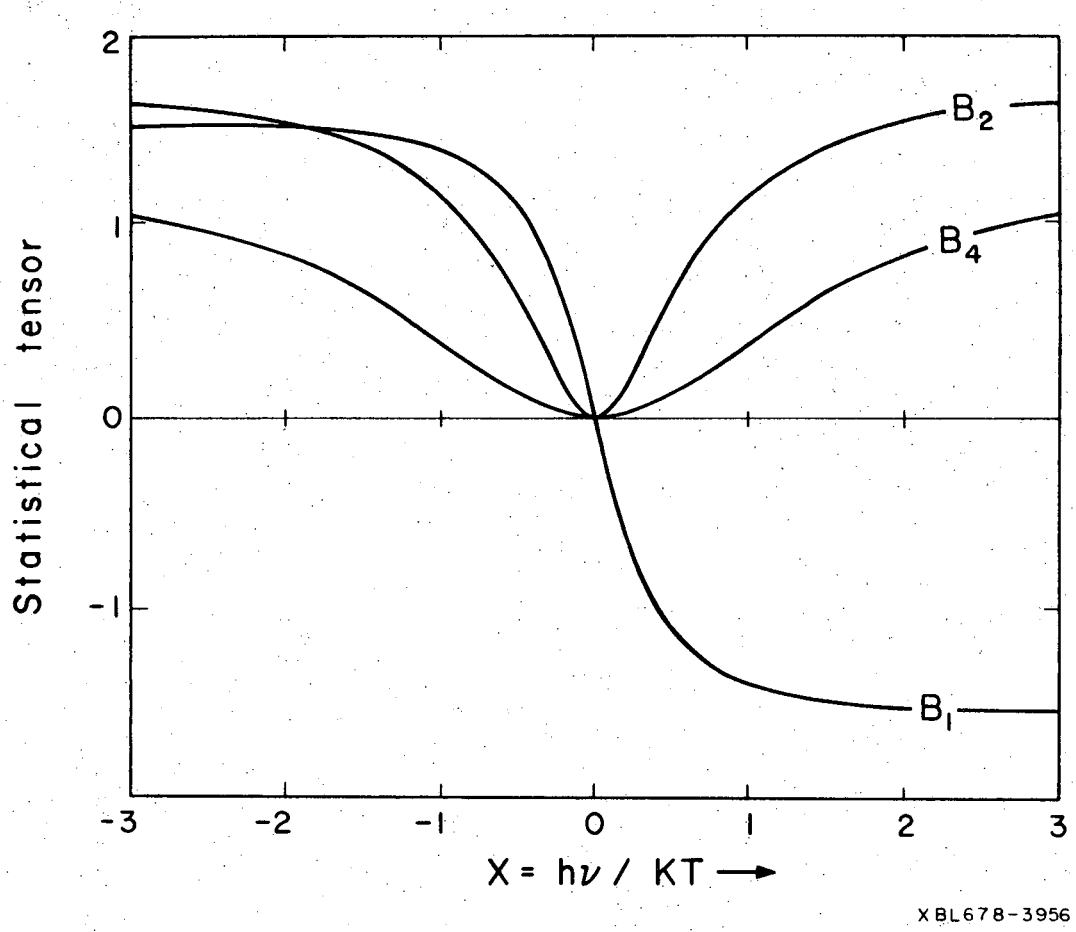

Fig. 8

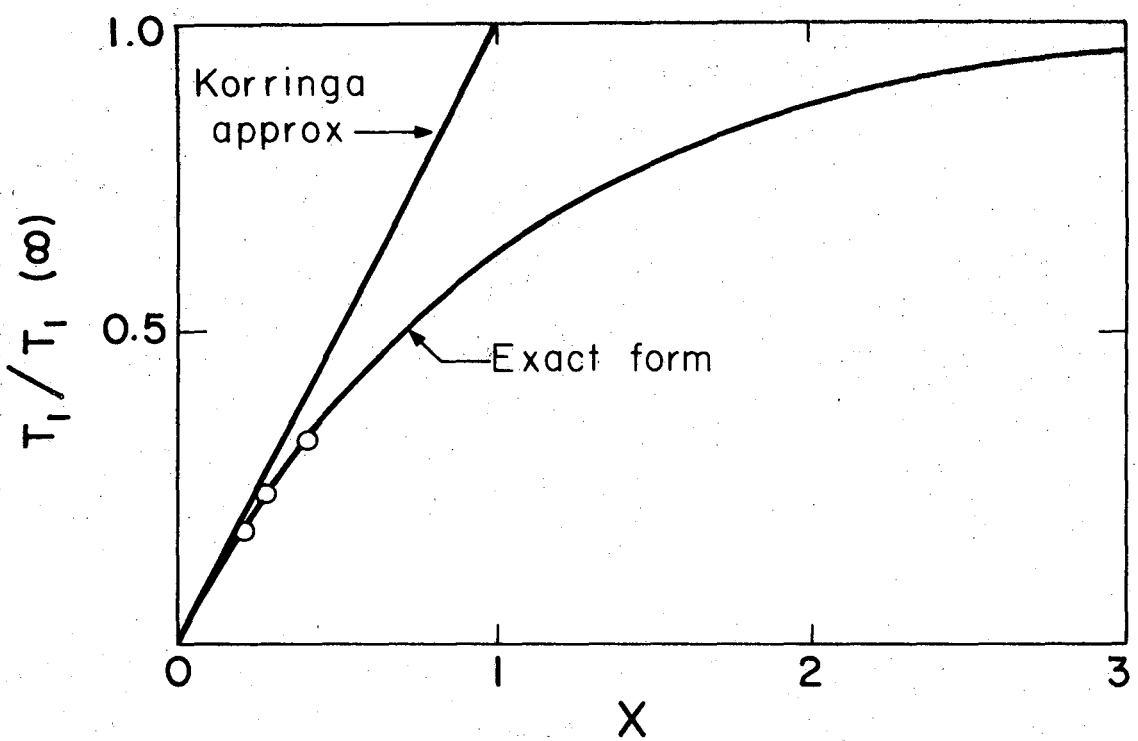

XBL678-3955

Fig. 9

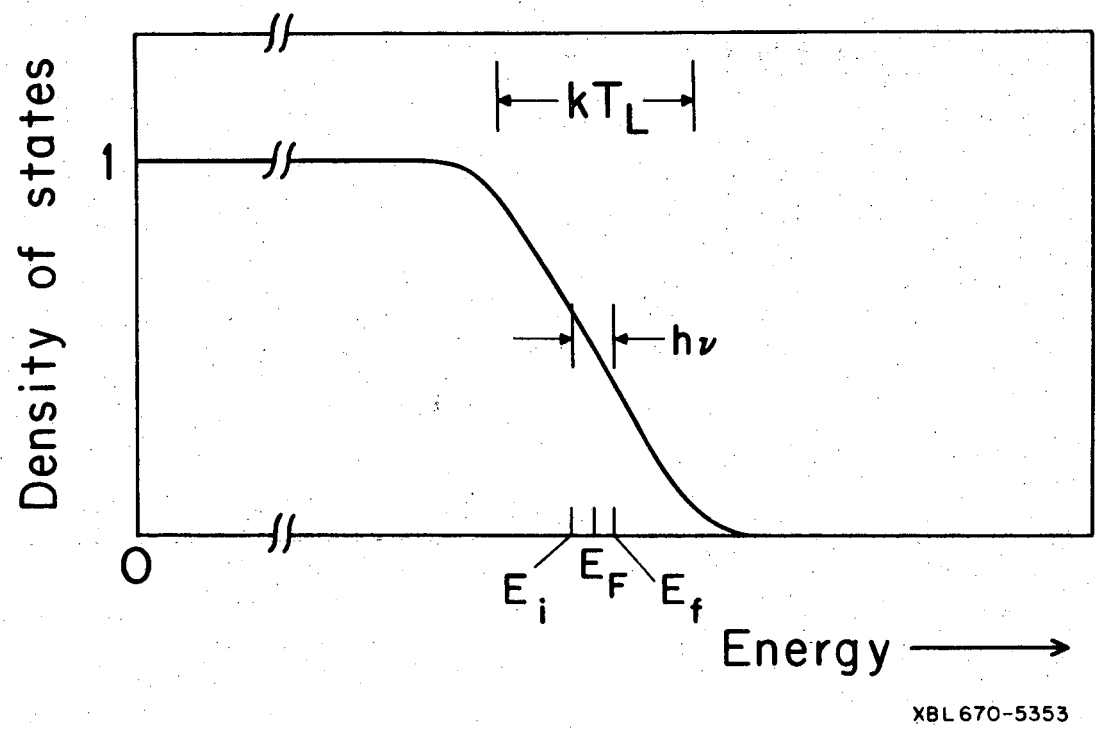

Fig. 10

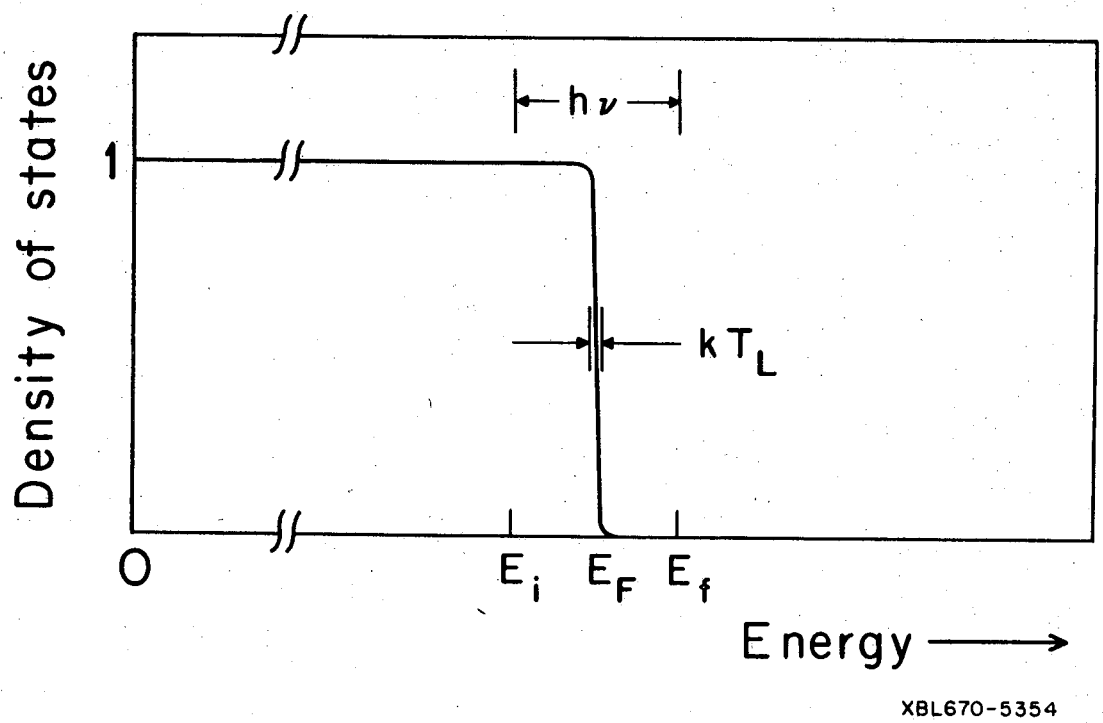

Fig. 11

This report was prepared as an account of Government sponsored work. Neither the United States, nor the Commission, nor any person acting on behalf of the Commission:

A. Makes any warranty or representation, expressed or implied, with respect to the accuracy, completeness, or usefulness of the information contained in this report, or that the use of any information, apparatus, method, or process disclosed in this report may not infringe privately owned rights; or

B. Assumes any liabilities with respect to the use of, or for damages resulting from the use of any information, apparatus, method, or process disclosed in this report.

As used in the above, "person acting on behalf of the Commission" includes any employee or contractor of the Commission, or employee of such contractor, to the extent that such employee or contractor of the Commission, or employee of such contractor prepares, disseminates, or provides access to, any information pursuant to his employment or contract with the Commission, or his employment with such contractor.